

# Kinetics of Resin-Supported Mitsunobu Esterification and Etherification Reactions

Xifeng Ma,<sup>†</sup> Ranran Shi,<sup>†</sup> Bin Zhang,<sup>†</sup> and Bing Yan<sup>\*,†,‡</sup>

School of Pharmaceutical Sciences, Shandong University, Jinan, China, and St. Jude Children's Research Hospital, Memphis, Tennessee 38105

Received January 9, 2009

Solid-phase Mitsunobu reaction is very useful in organic and parallel synthesis. In this work, we optimize the solid-phase Mitsunobu esterification and etherification reactions and investigated their kinetics by single-bead FTIR microspectroscopy method. Thirteen solid-phase Mitsunobu esterification reactions proceeded at rates between  $2.5 \times 10^{-3}$  and  $19 \times 10^{-3} \text{ s}^{-1}$ , while five etherification reactions at generally slower rates between  $3.3 \times 10^{-3}$  and  $8.9 \times 10^{-3} \text{ s}^{-1}$ . We discovered that reaction rates, as in solution phase Mitsunobu reactions, linearly correlated to  $\text{p}K_{\text{a}}$  values of acids and phenols used in the reaction. By studying side reactions and intermediates, we found that the solid-phase reaction mechanism also bears remarkable similarities to that of solution phase Mitsunobu reaction.

## Introduction

In the past 15 years, solid-phase organic synthesis (SPOS)<sup>1</sup> has played an indispensable role in combinatorial or diversity-oriented synthesis.<sup>2</sup> In recent surveys, SPOS accounts for nearly half of the compound libraries synthesized.<sup>2a–d</sup> New solution phase reactions are now actively investigated to transfer them to solid phase. However, optimization of solid-phase reaction conditions is not a trivial task. We have been engaged in such optimizations including studying reaction kinetics,<sup>3a–c</sup> key reaction steps,<sup>3e,f</sup> and real-time monitoring of the reaction progression<sup>3a,g,11</sup> using single-bead FTIR microspectroscopy<sup>3</sup> (single-bead IR) and other analytical techniques.<sup>3h</sup>

In solution, the Mitsunobu reaction<sup>4</sup> has gained wide acceptance in organic synthesis because of its effectiveness and versatility. This mild reaction converts a hydroxyl group into a potent leaving group that is able to be displaced by a wide variety of nucleophiles. However, the purification of reaction products from reagents and byproducts remains a major challenge.<sup>5</sup> Solid-phase Mitsunobu reaction<sup>6–10</sup> has also been applied in libraries synthesis. We noticed that the reaction conditions employed in those syntheses are not consistent and the kinetics and mechanism of solid-phase Mitsunobu reaction have not been reported. As part of our efforts to optimize SPOS, we set to investigate solid-phase Mitsunobu reaction kinetics and optimize the reaction conditions. We aimed to investigate the effects of various reaction conditions on the reaction kinetics, intermediates, and side reactions, not focus on cleaving the final products in the current study. To simplify the procedures, we skipped

the linker step and directly used Wang resin as an alcohol reactant for such investigations. We found that resin-supported Mitsunobu esterification reactions proceed faster than etherification reactions and the rate constants depended on  $\text{p}K_{\text{a}}$  of acids and phenols. Similarities between solid-phase and solution-phase Mitsunobu reactions were revealed by their common intermediate, side reactions, and reactant  $\text{p}K_{\text{a}}$  dependence.

## Results and Discussion

**Model Esterification Reaction.** We first investigated a reaction between Wang resin and benzoic acid (**2a** in Table 1) (Scheme 1) to select the reaction solvent, test the order of reagents addition, and optimize the reagent excess ratio. We selected  $\text{CH}_2\text{Cl}_2$  as the reaction solvent for its good resin swollen property and optimal reaction rate after testing nine solvents (benzene, DMF, THF,  $\text{CH}_2\text{Cl}_2$ ,  $\text{CHCl}_3$ , DMAC, DMSO, dioxane, pyridine). Different reagent addition orders were compared. The optimized protocol was to add compound **2a** to the swollen resin, followed by the addition of mixture of DIAD and  $\text{Ph}_3\text{P}$ . The reagent ratio was also compared. The optimum reagent excess was 10 equiv of acid, DIAD, and  $\text{Ph}_3\text{P}$ . The whole reaction mixture was stirred on an orbital shaker, and a drop of resin at various times was taken for analysis of the product conversion.

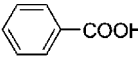
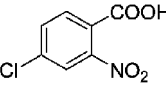
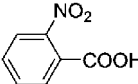
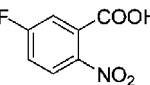
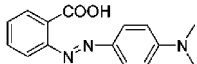
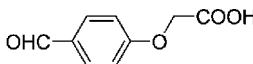
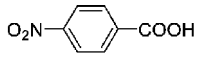
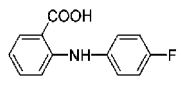
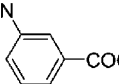
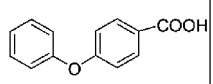
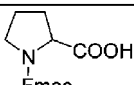
We used single-bead FTIR microspectroscopy to investigate the reaction time course on solid support. Despite typical polystyrene bands are evident in IR spectra, the distinctive band from the starting resin ( $3300 \text{ cm}^{-1}$ ) and the product ( $1718 \text{ cm}^{-1}$ ) are observed. An increasing IR peak at  $1718 \text{ cm}^{-1}$  indicated the formation of the product while the band at  $3300 \text{ cm}^{-1}$  from the starting alcohol (Wang resin) decreased as the reaction proceeded. FTIR spectra showing starting resin/product conversion at various times during the reaction are plotted in Figure 1 (A). The peak areas of the ester and alcohol bands at

\* To whom correspondence should be addressed. E-mail: bing.yan@stjude.org. Phone: +9014952797. Fax: +9014955715. Address: Department of Chemical Biology and Therapeutics, St. Jude Children's Research Hospital, 332 North Lauderdale Street, Memphis, TN, 38105.

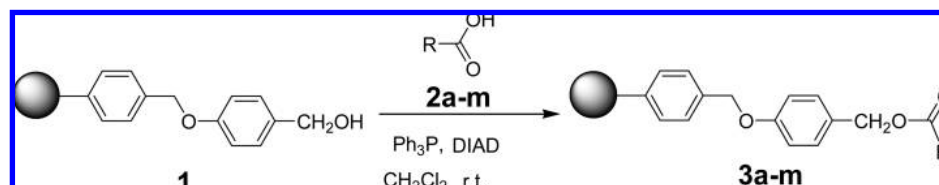
<sup>†</sup> Shandong University.

<sup>‡</sup> St. Jude Children's Research Hospital.

**Table 1.** Summary of IR Characteristics and Rate Constants

Entry	RCOOH (2a-m)	pKa (H <sub>2</sub> O)	Product (3a-m)	O=C str.(1/cm)	Rate Constant(s <sup>-1</sup> )
2a		4.20 <sup>a</sup>	3a	1718	7.91x10 <sup>-3</sup>
2b		1.26 <sup>b</sup>	3b	1736	18.7x10 <sup>-3</sup>
2c		2.18 <sup>a</sup>	3c	1736	19.3x10 <sup>-3</sup>
2d		2.46 <sup>b</sup>	3d	1739	15.1x10 <sup>-3</sup>
2e	ClCH <sub>2</sub> COOH	2.87 <sup>a</sup>	3e	1758	17.5x10 <sup>-3</sup>
2f		2.9 <sup>b</sup>	3f	1724	8.36x10 <sup>-3</sup>
2g		3.2 <sup>b</sup>	3g	1759	13.4x10 <sup>-3</sup>
2h		3.44 <sup>a</sup>	3h	1724	12.8x10 <sup>-3</sup>
2i		4.15 <sup>b</sup>	3i	1683	6.78x10 <sup>-3</sup>
2j		4.79 <sup>a</sup>	3j	1716	5.23x10 <sup>-3</sup>
2k		4.52 <sup>a</sup>	3k	1716	4.98x10 <sup>-3</sup>
2l	CH <sub>3</sub> COOH	4.76 <sup>a</sup>	3l	1739	2.51x10 <sup>-3</sup>
2m		4.87 <sup>b</sup>	3m	1745	2.44x10 <sup>-3</sup>

<sup>a</sup> Note: pKa (H<sub>2</sub>O) values were obtained by experimental<sup>14</sup> methods. <sup>b</sup> Note: pKa (H<sub>2</sub>O) values were obtained by calculated<sup>15</sup> methods.

**Scheme 1.** Reaction between Wang Resin and Acid

various times were integrated and the ratio of these peak areas to the peak area of an internal reference peak from polystyrene resin at 1947 cm<sup>-1</sup> was calculated and plotted against time. The kinetics data for solid-phase Mitsunobu reaction were fitted well to a pseudo-first-order<sup>3b,g,11d</sup> reaction rate equation (Figure 1B). The synthesis reached completion in 10 min. The depletion of alcohol and the formation of ester proceeded at a similar rate (7.83 and

7.91 × 10<sup>-3</sup> s<sup>-1</sup>) suggesting that there was no detectable side reactions.

**Kinetics of Esterification Reactions.** When the reaction conditions obtained above were applied, twelve carboxylic acids with electron-withdrawing, electron-donating, and sterically hindered functional groups were studied in solid-phase Mitsunobu reaction. FTIR spectra from these twelve reactions are shown in Figure 2. Peak area integration and

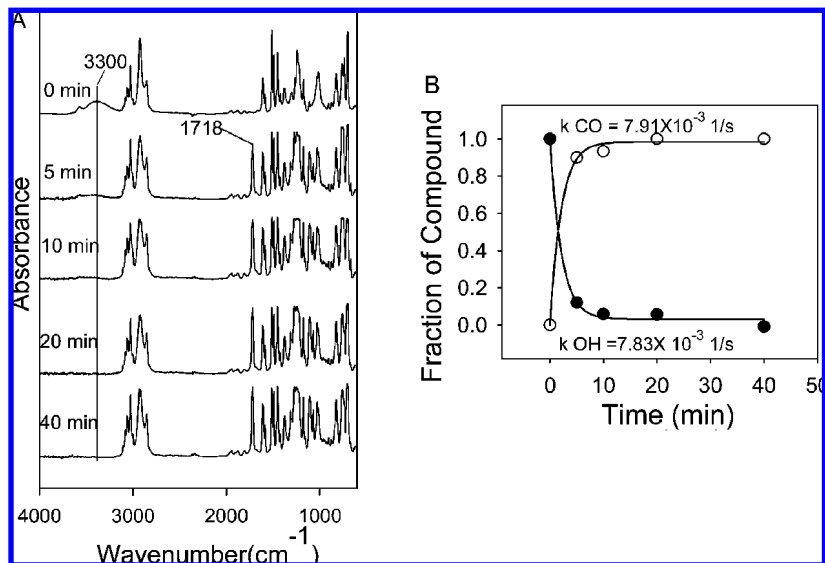


**Figure 1.** (A) Single-bead FTIR spectra showing the starting resin/product conversion at various times during the reaction. (B) The ratio of starting resin (●) and product (○) peak areas to the peak area of the internal reference band from the resin at 1947 cm<sup>-1</sup> was plotted against time. The line represents the best fit following a pseudo-first-order reaction rate equation with rate constants listed.

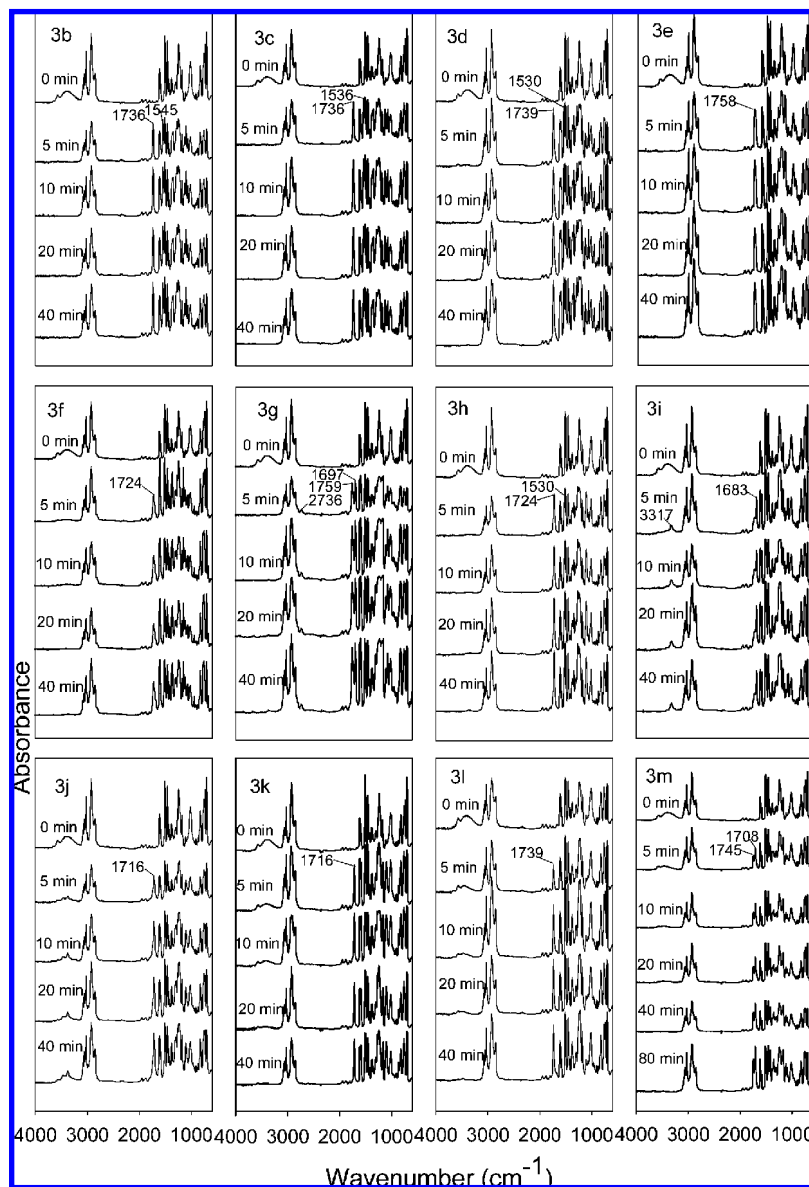


**Figure 2.** IR spectra showing 2b–m to 3b–m conversion at various times during the reaction.

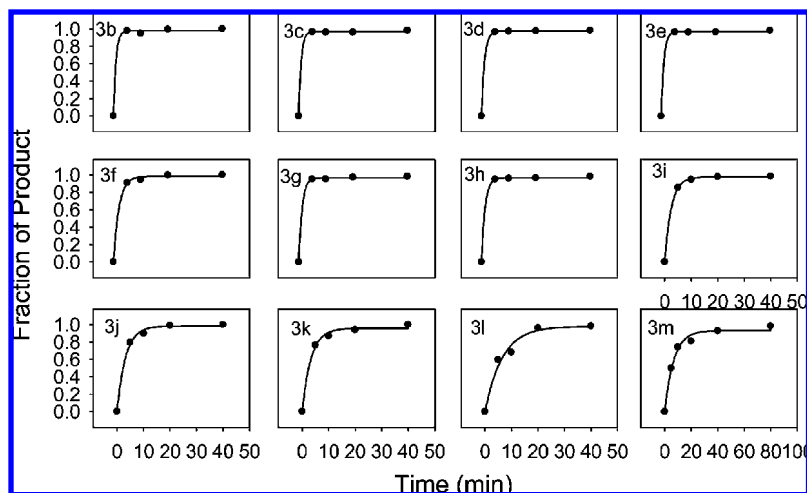


**Figure 3.** Time courses of the reactions for **3b–m** obtained by integrations of the carbonyl bands. Lines represent their pseudo-first-order best fit.

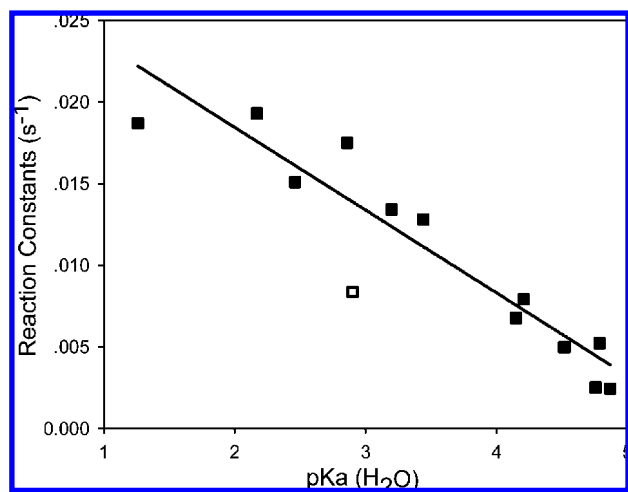


**Figure 4.** Plot of rate constants vs  $pK_a$  ( $H_2O$ ) values. Acid **2f** ( $\square$ ) showed slower rate because of steric hindrance.

kinetics analysis were carried out in the same way as in the model reaction study. The time courses of all reactions and the curve-fit results are shown in Figure 3, and the kinetics results are listed in Table 1.

To establish the relationship between  $pK_a$  values and reaction rates, we obtained experimental  $pK_a$  values from literature or calculated other values using SciTegic Pipeline Pilot (Accelrys, San Diego, CA). Kinetics analysis results showed that the acids with electron-withdrawing groups (therefore lower  $pK_a$ ) such as  $NO_2$ , Cl, and F reacted faster (Table 1). For example, the  $pK_a$  value of  $ClCH_2COOH$  (**2e**) is 2.87 and  $CH_3COOH$  (**2i**) is 4.76, and the rate constant for  $ClCH_2COOH$  is 7 times higher than that of  $CH_3COOH$ . The acids with electron-donating groups such as  $NH_2$  reacted slower.

A plot of  $pK_a$  ( $H_2O$ ) values<sup>14,15</sup> of acids versus the rate constants (Figure 4) shows a linear relationship. The regression coefficient is 0.953. An outlier was **2f** that reacted slowly probably caused by the steric hindrance in this molecule. Reactant **2i** also has similar steric hindrance as **2f**. However, because of its electronic properties, it is a weaker acid, and therefore, its slower reaction rate followed the linear trend of the  $pK_a$ - $k$  correlation. The rate-determining step of the Mitsunobu reaction is an  $S_N2$  displacement on the carbon

atom next to the alcohol group by a nucleophile, a carboxylate anion. Therefore, stronger acids reacted faster and the  $pK_a$  values have a profound effect on the reaction rate as in solution Mitsunobu reaction.<sup>12b</sup>

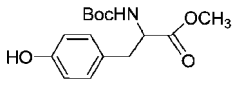
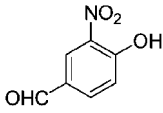
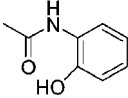
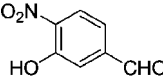
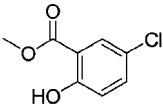
Acids with very low  $pK_a$  values ( $pK_a$  1–3) reacted too fast to have their kinetics feature differentiated. To better study their reaction rates, we lowered the reagent excess to six equivalents of acid,  $Ph_3P$  and DIAD. Their rate constants were much better differentiated and the rates also showed a linear relationship with  $pK_a$  values (see Supporting Information).

**Model Etherification Reaction.** The Mitsunobu etherification is also a useful reaction for organic and library synthesis. First, we used Wang resin and Boc-tyrosine-ester (**4a** in Table 2) to optimize the reaction conditions (Scheme 2).  $CHCl_3$  was found to be the best reaction solvent for solid phase Mitsunobu etherification reaction after testing seven solvents (DMF, THF,  $CH_2Cl_2$ ,  $CHCl_3$ , DMSO, dioxane, pyridine). The optimized protocol was to add compound **4a** to the swollen resin, followed by the addition of mixture of DIAD and  $Ph_3P$ , and the mixture was stirred on an orbital shaker. The optimum ratio was to use 10 equiv of phenol and 20 equiv of DIAD and  $Ph_3P$ .

All phenols used in this study were selected to contain an extra carbonyl group as a spectroscopic marker so that the formation of Mitsunobu products can be conveniently monitored by single bead FTIR microspectroscopy. An increasing peak at  $1744\text{ cm}^{-1}$  in IR spectra indicated the formation of the product for the model reaction. FTIR spectra showing the starting resin/product conversion at various times during the reaction are shown in Figure 5A. Intensities of IR bands corresponding to two carbonyl groups ( $1744$  and  $1716\text{ cm}^{-1}$ ) increased with time and the IR band for the hydroxyl group ( $3300\text{ cm}^{-1}$ ) from the starting resin decreased. The latter was converted to an IR band corresponding to  $-NH-$  group (Figure 5A). The synthesis reached completion in 20 min with a rate constant of  $3.97 \times 10^{-3}\text{ s}^{-1}$ .

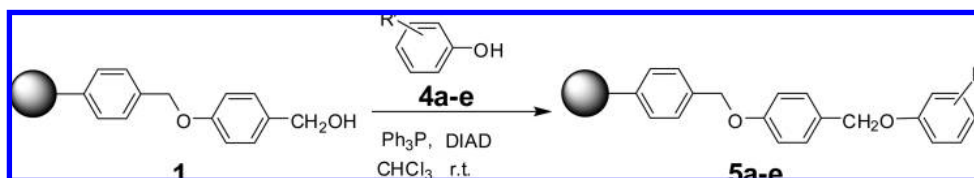
**Kinetics of Etherification Reactions.** When the reaction conditions obtained in the model reaction studies were applied, four other etherification reactions were investigated using phenols with different  $pK_a$  values. FTIR spectra (Figure 6) and

**Table 2.** Summary of IR Characteristics and Rate Constants<sup>a</sup>

Entry	Ph-OH	pKa(H <sub>2</sub> O)	Product	O=C str.(1/cm)	Rate Constants(s <sup>-1</sup> )
4a		10.37	5a	1744	3.97 × 10 <sup>-3</sup>
4b		4.61	5b	1700	5.85 × 10 <sup>-3</sup>
4c		7.65	5c	1693	3.42 × 10 <sup>-3</sup>
4d		6.93	5d	1705	3.30 × 10 <sup>-3</sup>
4e		9.36	5e	1731	2.29 × 10 <sup>-3</sup>

<sup>a</sup> Note: pKa (H<sub>2</sub>O) values were obtained by calculation.<sup>15</sup>

### Scheme 2. Reaction between Wang Resin and Phenols



reaction time courses (Figure 7) were obtained using the same protocol as above. The summary of IR characteristics and rate constants is listed in Table 2. Analysis showed that the reaction rates have a linear relationship with the pK<sub>a</sub> values of phenols (Figure 8) demonstrating that the rate of Mitsunobu etherification also depends on the acidity of phenols.

**Reaction Intermediate and Possible Side Reactions.** The mechanism of Mitsunobu reaction in solution has been

thoroughly investigated.<sup>4d,12,16</sup> However, the mechanism on solid phase, like the reaction kinetics, has not been reported. In the following, we present some of our observations that may suggest a plausible reaction mechanism on resin support (Scheme 3).

After mixing the DIAD-Ph<sub>3</sub>P adduct with the swollen resin, we observed double peaks at 1739 and 1712 cm<sup>-1</sup> that are attributed to two different C=O groups in intermediate

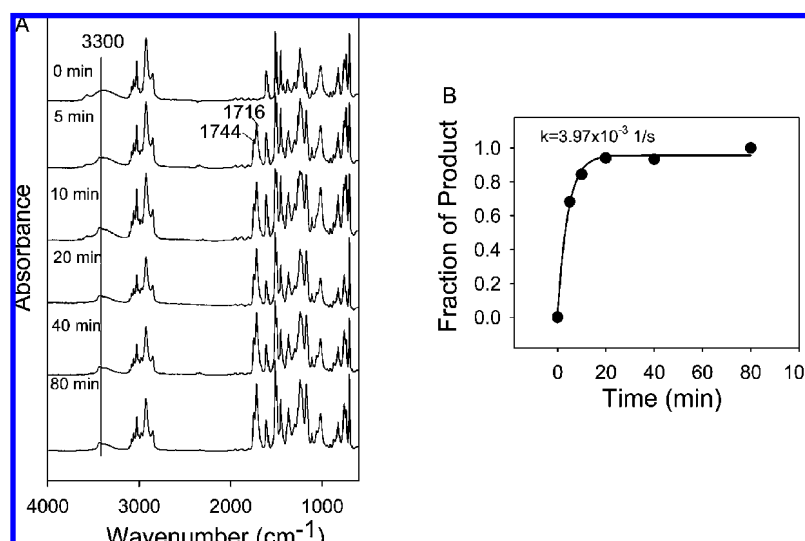


**Figure 5.** (A) FTIR spectra showing the starting resin/product conversion at various times during the model reaction. (B) Time course of the model reaction. The line represents the best fit following a pseudo-first-order reaction rate equation.

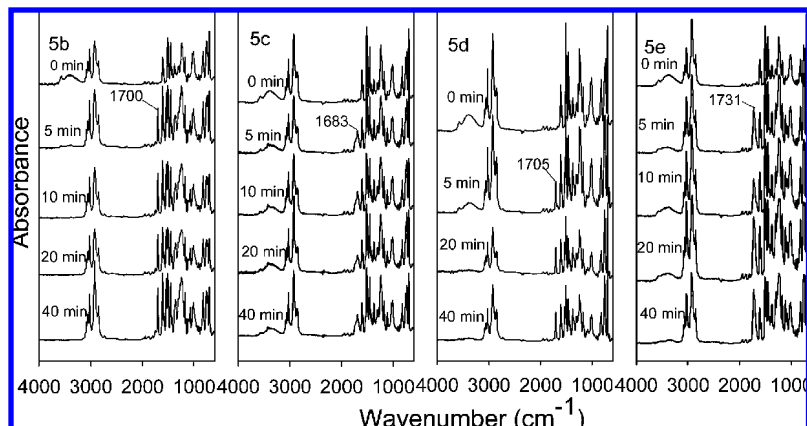


Figure 6. IR spectra showing **4b–e** to **5b–e** conversions at various times during the reaction.

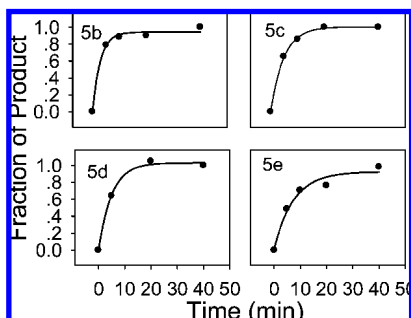


Figure 7. Time courses of the reactions of **4b–e** to **5b–e** conversions and their best fits to a first-order reaction rate equation (lines).

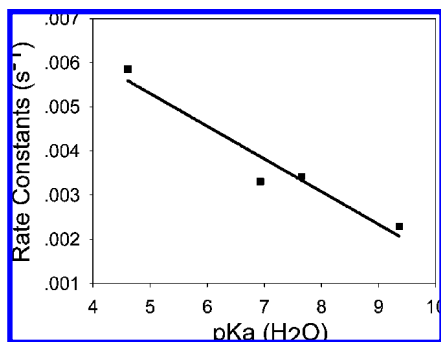


Figure 8. Plot of rate constants of phenols vs their  $pK_a$  ( $H_2O$ ) values.<sup>15</sup>

**11** (Figure 9A). Another piece of evidence is that IR band for hydroxyl group at  $3310\text{ cm}^{-1}$  from the starting resin disappeared, and it was converted to an IR band that could be attributed to the  $-NH-$  group (Figure 9A). Further supporting evidence is that the nitrogen content of the starting Wang resin is 0.004% while the adduct 2.66% based on element analysis. The rate constant for the formation of the intermediate **11** is  $2.29 \times 10^{-3}\text{ s}^{-1}$  (Figure 9B). This suggests that if there is no acid or phenol when the alcohol is activated, DIAD will attack the alcohol and form the undesired product **11**. Actually, we observed more side product **11** when the addition of acid was delayed in some of our early experiments. To optimize the product formation and avoid this side reaction, we added the acid to resins before the addition of DIAD- $Ph_3P$  adduct. This practice seemed to effectively prevent the side reaction and afford product formation. The

formation of **11** is not surprising because similar adduct has previously been identified in solution reactions.<sup>13</sup>

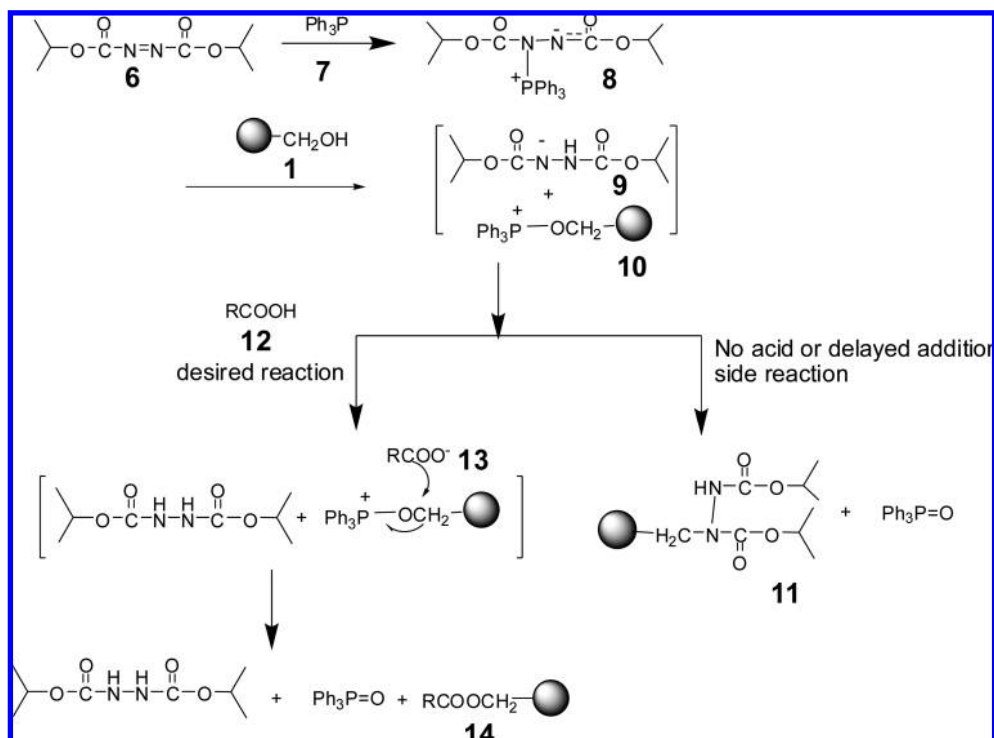
## Summary

Solid-phase Mitsunobu reaction is a powerful method in organic and combinatorial synthesis. In this work, we optimized solid-phase Mitsunobu esterification and etherification reactions and generated the first report on their kinetics investigation. Solid-phase Mitsunobu esterification reactions proceeded at rates between  $2.5 \times 10^{-3}$  and  $19 \times 10^{-3}\text{ s}^{-1}$ , while etherification occurred at generally slower rates between  $3.3 \times 10^{-3}$  and  $8.9 \times 10^{-3}\text{ s}^{-1}$ . We discovered that reaction rates linearly correlated to  $pK_a$  values of acids and phenols used in the reaction. The solid-phase reaction mechanism bears remarkable similarities to the solution-phase Mitsunobu reaction. We found that the transiently formed strong leaving group on the alcohol may be under attack by DIAD if the acids/phenols are not available. Therefore, early addition of the reactant (acid/phenol) is essential for high yield and purity of the product. We were also convinced that swollen resin behaved just like another reaction solvent<sup>17</sup> in its effects on the reaction. The optimized reaction conditions and the better understanding of the reaction kinetics and mechanism have provided valuable information for organic synthesis and combinatorial or diversity-oriented synthesis on resin supports.

## Experimental Section

**Materials.** Wang resin was purchased from Advanced ChemTech (Louisville, Kentucky), and reagents were purchased from Sigma-Aldrich (St. Louis, MO). They were used without further purification. Wang resin was 100–200 mesh with a loading of 1.26 mmol/g.

**General Procedure of Mitsunobu Esterification Reaction.** All reactions were performed in 3 mL SPE filtration tubes. Wang resin (10 mg) was swollen in  $CH_2Cl_2$  for 20 min and drained. DIAD (10 equiv) in 0.5 mL  $CH_2Cl_2$ ,  $Ph_3P$  (10 equiv) in 0.5 mL  $CH_2Cl_2$ , and RCOOH (10 equiv) in 0.5 mL  $CH_2Cl_2$  were used. DIAD was added dropwise to  $Ph_3P$  over three minutes. RCOOH was added to the swollen resin first. Then DIAD- $Ph_3P$  was added to the mixture, and the mixture was stirred on an orbital shaker. At various times, a droplet of resin was taken and washed with THF and

**Scheme 3.** Postulated Mechanism of the Mitsunobu Reaction on Resin Support

$\text{CH}_2\text{Cl}_2$  five times each. The resin was air-dried for FTIR microspectroscopy measurements.

**General Procedure of Mitsunobu Etherification Reaction.** Wang resins (10 mg) were swollen in  $\text{CH}_2\text{Cl}_2$  for 20 min and drained. DIAD (20 equiv) in 0.5 mL  $\text{CHCl}_3$ ,  $\text{Ph}_3\text{P}$  (20 equiv) in 0.5 mL  $\text{CHCl}_3$ , and phenols (10 equiv) in 0.5 mL  $\text{CHCl}_3$  were used for the reaction. DIAD was added dropwise to  $\text{Ph}_3\text{P}$  over three minutes. Phenol (10 equiv) was added to the swollen resin first, and then the DIAD- $\text{Ph}_3\text{P}$  adduct was added to the resin slurry. The whole mixture was stirred on an orbital shaker. At various times, a droplet of resin was taken and washed with THF and  $\text{CH}_2\text{Cl}_2$  for 5 times each. The resin was air-dried for FTIR microspectroscopy measurements.

**Single-Bead FTIR Microspectroscopy.** All spectra were collected on a Nicolet 380 FT-IR spectrophotometer (Thermo Fisher Scientific, Waltham, MA) coupled with a continuum microscope. The system was operated by the OMNIC software. The microscope was equipped with a  $100\times$  Cassegrain objective and a liquid nitrogen-cooled mercury cadmium-telluride (MCT) detector. The resin beads were flattened in a NaCl window. The view mode aided in the location of a single flattened bead, and the transmission mode was used for the measurement. A clean area on the NaCl window next to the bead was used to collect the background spectrum. Data were collected at  $4\text{ cm}^{-1}$  resolution, and 200 scans were averaged.

**Data Analysis.** To correct peak area variations cause by factors such as variations in bead size, the thickness of

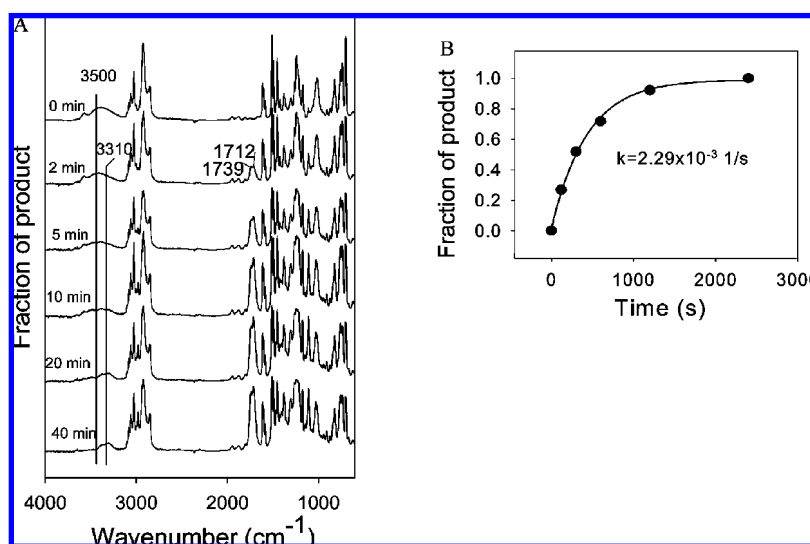


**Figure 9.** (A) IR spectra showing the intermediate **11** formation at various time during the reaction. (B) The time courses of the reaction. The line represents the best fit following a pseudo-first-order reaction rate equation.

flattened bead, and the random fluctuation of the instrument, we used an IR band of polystyrene at  $1947\text{ cm}^{-1}$  as an internal reference peak. The ratio of the integrated peak area to the internal reference peak area in the same measurement was used to quantify the reaction conversion and plotted against time for kinetic analysis. These data points were fitted to a pseudo-first-order rate equation<sup>11</sup> by using nonlinear regression analysis with SigmaPlot for windows 10.0 (Systat Software Inc., Richmond, CA) on a personal computer.

**Acknowledgment.** We thank Hongyu Zhou for technical assistance. This work was supported by National Basic Research Program of China (973 Program 2009CB930103), the American Lebanese Syrian Associated Charities (ALSAC), and St. Jude Children's Research Hospital.

**Supporting Information Available.** Kinetics data including IR spectra and data analysis for four strong acids at a reduced reagent excess (6-fold excess). This material is available free of charge via the Internet at <http://pubs.acs.org>.

## References and Notes

- (1) (a) Leznoff, C. C. *Acc. Chem. Res.* **1978**, *11*, 327–333. (b) Akelah, A.; Sherrington, D. C. *Chem. Rev.* **1981**, *81*, 557–587. (c) Frechet, J. M. J. *Tetrahedron* **1981**, *37*, 663–683. (d) Hodge, P. In *Synthesis and Separations Using Functional Polymers*; Sherrington, D. D., Hodge, P., Eds.; Wiley: Chichester, U.K., 1988; Chapter 2.
- (2) (a) Dolle, R. E.; Le Bourdonnec, B.; Goodman, A. J.; Morales, G. A.; Salvino, J. M.; Zhang, W. *J. Comb. Chem.* **2007**, *9*, 855–902. (b) Dolle, R. E.; Le Bourdonnec, B.; Morales, G. A.; Moriarty, K. J.; Salvino, J. M. *J. Comb. Chem.* **2006**, *8*, 597–635. (c) Dolle, R. E. *J. Comb. Chem.* **2005**, *7*, 739–798. (d) Dolle, R. E. *J. Comb. Chem.* **2004**, *6*, 623–679. (e) Gordon, E. M.; Barrett, R. W.; Dower, W. J.; Fodor, S. P. A.; Gallop, M. A. *J. Med. Chem.* **1994**, *37*, 1385–1401. (f) Thompson, L. A.; Ellman, J. A. *Chem. Rev.* **1996**, *96*, 555–600. (g) DeWitt, D. H.; Czarnik, A. W. *Acc. Chem. Res.* **1996**, *29*, 114–122. (h) Balkenhohl, F.; Ussche-Hunnefeld, C.; Lansky, A.; Zechel, C. *Angew. Chem., Int. Ed. Engl.* **1996**, *35*, 2288–2337. (i) Lam, K. S.; Lebl, M.; Krchnak, V. *Chem. Rev.* **1997**, *97*, 411–448. (j) Hergenrother, P. J.; Depew, K. M.; Schreiber, S. L. *J. Am. Chem. Soc.* **2000**, *122*, 7849–7850. (k) MacBeath, G.; Koehler, A. N.; Schreiber, S. L. *J. Am. Chem. Soc.* **1999**, *121*, 7967–7968.
- (3) (a) Yan, B.; Kumaravel, G.; Anjaria, H.; Wu, A.; Petter, R.; Jewell, C. F.; Wareing, J. R. *J. Org. Chem.* **1995**, *60*, 5736–5738. (b) Yan, B.; Fell, J. B.; Kumaravel, G. *J. Org. Chem.* **1996**, *61*, 7467–7472. (c) Yan, B. *Acc. Chem. Res.* **1998**, *31*, 621–630. (d) Yan, B.; Shi, R.; Zhang, B.; Kshirsagar, T. *J. Comb. Chem.* **2007**, *9*, 684–689. (e) Yan, B.; Nguyen, N.; Liu, L.; Holland, G.; Raju, B. *J. Comb. Chem.* **2000**, *2*, 66–74. (f) Fang, L.; Demee, M.; Sierra, T.; Kshirsagar, T.; Celebi, A.; Yan, B. *J. Comb. Chem.* **2002**, *4*, 362–368. (g) Yan, B.; Sun, Q.; Wareing, J. R.; Jewell, C. F. *J. Org. Chem.* **1996**, *61*, 8765–8770. (h) Irving, M.; Cournoyer, J.; Li, R.; Santos, C.; Yan, B. *Comb. Chem. High Throughput Screening* **2001**, *4*, 353–362. (i) Yan, B.; Kumaravel, G. *Tetrahedron* **1996**, *52*, 843–848.
- (4) (a) Mitsunobu, O. *Synthesis* **1981**, *1*, 1–28. (b) Hughes, D. L. *Org. React.* **1992**, *42*, 335–656. (c) Hughes, D. L. *Org. Prep. Proc. Int.* **1996**, *28*, 127–164. (d) Mitsunobu, O. *Bull. Chem. Soc. Jpn.* **1967**, *40*, 2380–2382. (e) Fitzjarrald, V. P.; Pongdee, R. *Tetrahedron Lett.* **2007**, *48*, 3553–3557.
- (5) Lan, P.; Porco, J. A.; South, M. S.; Parlow, J. J. *J. Comb. Chem.* **2003**, *5*, 660–669.
- (6) For C–O ester bond formation, see: (a) Krchňák, V.; Cabel, D.; Weichsel, A. S.; Flegelova, Z. *Let. Pept. Sci.* **1995**, *2*, 277–282. (b) Barbaste, M.; Rolland-Fulcrand, V.; Roumestant, M.-L.; Viallefont, P.; Martinez, J. *Tetrahedron Lett.* **1998**, *39*, 6287–6290.
- (7) For C–O ether bond formation, see: (a) Valerio, R. M.; Bray, A. M.; Patsiouras, H. *Tetrahedron Lett.* **1996**, *37*, 3019–3022. (b) Vergnon, A. L.; Pottorf, R. S.; Playner, M. R. *J. Comb. Chem.* **2004**, *6*, 91–98. (c) Krchnak, V.; Flegelova, Z.; Weichsel, A. S.; Lebl, M. *Tetrahedron Lett.* **1995**, *36*, 6193–6196. (d) Rano, T.; Chapman, K. *Tetrahedron Lett.* **1995**, *36*, 3789–3792.
- (8) For C–N bond formation, see: (a) Chhabra, S. R.; Khan, A. N.; Bycroft, B. W. *Tetrahedron Lett.* **2000**, *41*, 1099–1102. (b) Zaragoza, F.; Stephensen, H. *Tetrahedron Lett.* **2002**, *43*, 1019–1021. (c) Esteve, C.; Vidal, B. *Tetrahedron Lett.* **2002**, *43*, 1019–1021. (d) Jeon, H. S.; Yoo, J. H.; Kim, J. N.; Kim, T. H. *Tetrahedron Lett.* **2007**, *48*, 439–441.
- (9) For C–C bond formation, see: Chaturvedi, S.; Otteson, K.; Bergot, J. *Tetrahedron Lett.* **1999**, *40*, 8205–8209.
- (10) For intramolecular bond formation, see: (a) Wang, F.; Hauske, J. R. *Tetrahedron Lett.* **1997**, *38*, 6529–6532. (b) Arya, P.; Wei, C. Q.; Barnes, M. L.; Daroszewska, M. *J. Comb. Chem.* **2004**, *6*, 65–72.
- (11) (a) Yan, B.; Gstach, H. *Tetrahedron Lett.* **1996**, *37*, 8325–8328. (b) Marti, R.; Yan, B.; Jarosinski, M. *J. Org. Chem.* **1997**, *62*, 5615–5618. (c) Yan, B.; Li, W. *J. Org. Chem.* **1997**, *62*, 9354–9357. (d) Li, W.; Yan, B. *J. Org. Chem.* **1998**, *63*, 4092–4097.
- (12) (a) Varasi, M.; Walker, K. A. M.; Maddox, M. L. *J. Org. Chem.* **1987**, *52*, 4235–4238. (b) Hughes, D. L.; Reamer, R. A.; Bergan, J. J.; Grabowski, E. J. *J. Am. Chem. Soc.* **1988**, *110*, 6487–6491.
- (13) (a) Dow, R. L.; Kelly, R. C.; Schletter, I.; Wierenga, W. *Synth. Commun.* **1981**, *11*, 43–53. (b) DiGrandi, M. J.; Tilley, J. W. *Tetrahedron Lett.* **1996**, *37*, 4327–4330.
- (14) Dean, J. A.; Lange, N. A. *Lange's Handbook of Chemistry*, 15th ed.; McGraw-Hill: New York, 2001.
- (15) The pKa values were calculated by SciTegic Pipeline Pilot software (Accelrys, San Diego, CA). The file containing the compound structure was firstly transferred to SDF file by Accord for Excel (Accelrys, San Diego, CA). The SDF file was then imported into Pipeline Pilot to calculate the pKa values using a calculation function in the software.
- (16) (a) Grochowski, E.; Kupper, R. J.; Michejda, C. J. *J. Am. Chem. Soc.* **1982**, *104*, 6876–6877. (b) Camp, D.; Jenkins, I. D. *J. Org. Chem.* **1989**, *54*, 3045–3049.
- (17) Czarnik, A. W. *Biotechnol. Bioeng. (Comb. Chem.)* **1998**, *61*, 77–79.

CC900004M